Chin. J. Astron. Astrophys. Vol. 6 (2006), No. 5, 579–587
(*http://www.chjaa.org*)

Chinese Journal of
Astronomy and
Astrophysics

High Resolution Spectroscopy of Halo Stars in the Near UV and Blue Region

I. Spectra in the Wavelength Region 3550–5000 Å*

V. G. Klochkova[1,2], Gang Zhao[1], S. V. Ermakov[1,2] and V. E. Panchuk[1,2]

[1] National Astronomical Observatories, Chinese Academy of Sciences, Beijing 100012
gzhao@bao.ac.cn
[2] Special Astrophysical Observatory, Russian Academy of Sciences, Nighnij Arkhyz, 369167
Karachai-Cherkessia, Russia

Received 2005 November 1; accepted 2006 April 10

Abstract An atlas of high resolution ($R = 60\,000$) CCD-spectra in the wavelength range 3500–5000 Å is presented for four objects in metallicity range $-3.0 < [\mathrm{Fe/H}] < -0.6$, temperature range $4750 < T_{\mathrm{eff}} < 5900$ K, and surface gravity range $1.6 < \lg g < 5.0$. We describe the calibration of the stellar atmospheric parameters using Alonso's formula based on the method of infrared flux and outline the determination of the abundances of a total number of 25 chemical elements. An analysis of the abundance determination errors for different chemical elements is carried out, and a method is provided for the observations and reduction of spectral material. Properties of the method of producing an atlas of spectra and line identifications are described.

Key words: stars: halo stars – stars: G, K-type – stars: spectra – stars: UV-spectra

1 INTRODUCTION

Metal-poor stars in the Galactic halo provide us with information on the first generation of stars and nucleosynthesis events associated with them. The spectroscopic study of the halo stars can present the chemical evolution of early history and kinematic structure of our Galaxy (e.g. Beers & Christlieb 2005; Zhao et al. 2006). Simulations of the early inhomogeneous Galactic halo show that the distributions of metal-poor stars in the correlation diagrams are insensitive to any parameter other than what the supernova yields. Specific variations in the yields produce certain stellar patterns in the diagrams. Thus, we can distinguish theoretical yield calculations merely by studying these patterns. The spectra of halo stars in the near-UV and blue region contain many heavy element lines, which can provide us the information of the abundance patterns, the Galactic chemical evolution at early stage, and the nucleosynthesis of the supernova type II as well.

This paper presents a comparative description of the near-UV and blue region optical spectra of four halo stars with different metallicities. The results were obtained through a general study of low mass F–K-type metal poor stars in the Galactic halo. This paper includes a detailed comparison of the spectra of stars within the same category and among different categories which may help to distinguish metal deficient stars in the search for new spectroscopic criteria. In this connection several spectroscopic features are particularly interesting, for instance, some spectra could be useful for studies of the chemical abundances of stars and determination of their evolution stages, etc. Furthermore, the atlas provides a spectral library for population synthesis.

* Supported by the National Natural Science Foundation of China.

2 OBSERVATIONS AND DATA REDUCTION

The stars selected for the atlas are chosen to cover the widest range in metallicity. Aiming to obtain high resolution and high signal to noise ratio spectra, we chose stars of bright visual magnitudes (the faintest star in our list is HD 115444 with $V = 8.98^{\rm m}$). Some basic data of the stars and their model parameters adopted in this study are presented in Table 1. The successive columns are: star name, visual magnitude, color index $b-y$, c_1, parallax, error of parallax, effective temperature, gravity, metallicity and turbulent velocity. The observations were done at the 6-m telescope of the Special Astrophysical Observatory (SAO) of the Russian Academy of Sciences with the échelle-spectrograph NES (Nasmyth–2 focus, 2048×2048 CCD-chip, $R = 60\,000$) (Panchuk et al. 1999; Panchuk et al. 2002a; Panchuk et al. 2002b). The spectrograph NES has a fused silica camera which permits making spectral observations in the UV range.

Table 1 Basic Data and Model Atmospheric Parameters of the Program Stars

Star	V	$b-y$	$\rm m_1$	c_1	π	$\sigma(\pi)$	$T_{\rm eff}$	$\lg g$	[Fe/H]	ξ_t
					mas	mas	K			km s^{-1}
G27–44	7.411	0.355	0.119	0.306	23.66	0.97	5900	4.35	–0.60	1.0
HD 188510	8.832	0.416	0.107	0.148	25.32	1.17	5410	5.00	–1.52	0.6
G37–26	8.056	0.351	0.058	0.208	25.85	1.14	5890	4.50	–2.04	0.7
HD 115444	8.975	0.586	0.056	0.467	3.55	1.12	4800	1.60	–2.91	1.7

In order to remove cosmic ray traces and to increase the signal to noise ratio, at least two spectra of each star were observed. Cosmic ray traces were removed by median averaging of two subsequent spectra. A hollow cathode Th-Ar lamp was used for the wavelength calibration.

The 2D spectral data were reduced with the ECHELLE package of MIDAS (version 01FEB), which includes standard procedures of bias subtraction, scattering light and cosmic ray trace removal, and order extraction. Further measurements (photometric and positional) in the 1D spectra were made with the DECH20 package (Galazutdinov 1992). In particular, positions of the spectral lines were measured by matching the original and mirrored profiles. Instrumental corrections for the measured wavelength were tested via using telluric lines of oxygen and water.

The determination of continuum location in UV and blue wavelength ranges surrounded by numerous metallic lines demands a specially high accuracy. In order to achieve such high accurate measurement, we adopt a procedure comprising the following steps: comparison of continuum locations for the order with two nearest ones, comparison of spectral regions in overlapping orders, comparison of observed spectra with synthetic ones. The code STARSP (Tsymbal 1996) was used for calculation of synthetic spectra.

3 THE LIST OF LINES

The lines in the spectra were identified using the data from the VALD (Piskunov 1995; Kupka et al 1999; Ryabchikova et al 1999). The atomic parameters of lines needed for the chemical abundances calculation (oscillator strengths, damping constants, etc.) were taken from the same source. The initial list of lines includes about 8100 lines. A total of 860 unblended lines were selected based on the solar spectrum. In order to control the identification, we used the VALD list by Pierce & Breckinridge (1974). The first few rows of the list of lines reliably identified is given in Table 2. The whole Table 2 in electronic format is available at *http://www.chjaa.org/2006_6_5.htm*. Some of these lines show over-large errors in the chemical abundances caused by incorrect identification, blending, and wrong oscillator strengths. Such lines are marked by the colon ":" in Table 2, and were not taken into account in the final determination of chemical abundance. Most of the lines in the table have a low value of equivalent width which means that they are located in the linear part of the curve of growth and so are suitable for abundance calculations.

4 SPECTRAL ATLAS

The spectra of two stars over the whole spectral range are presented in Figure 1 to illustrate an effect of difference in metallicity. On such a scale where the Balmer lines (especially Hγ and Hβ) and the Ca II doublet are clearly seen, the role of blanketing effect is well illustrated.

Table 2 Equivalent Widths (E.W., mÅ) and Abundances $\lg \varepsilon(X)$ of Individual Lines

Element	λ, Å	$\lg gf$	E.W.	$\lg \varepsilon(X)$	E.W.	$\lg \varepsilon(X)$	E.W.	$\lg \varepsilon(X)$	E.W.	$\lg \varepsilon(X)$
			G27–44		HD188510		G37–26		HD115444	
Na 1	4497.657	–1.560	6.6	5.533	–	–	–	–	–	–
Na 1	4668.559	–1.300	14.9	5.657	–	–	–	–	–	–
Na 1	4982.814	–0.950	28.8	5.659	–	–	–	–	1.5	3.725
Mg 1	3832.304	0.121	–	–	–	–	–	–	191.7	5.066:
Mg 1	3838.292	0.392	–	–	–	–	–	–	211.9	4.928:
Mg 1	3986.753	–1.444	125.0	7.284	77.3	6.495	29.8	6.206	21.1	5.511
Mg 1	4057.505	–1.201	154.3	7.359	93.8	6.385	41.9	6.171	35.5	5.590
Mg 1	4165.101	–2.680	10.2	6.944	13.3	6.866:	–	–	–	–
Mg 1	4167.271	–1.004	148.0	7.229	113.7	6.346	52.2	6.134	41.1	5.500
Mg 1	4571.096	–5.691	70.5	7.071	66.0	6.232	16.2	5.973	53.6	5.238
Mg 1	4702.991	–0.666	158.0	6.787	144.7	6.038	73.8	5.951	56.2	5.373
Mg 1	4730.029	–2.523	27.0	7.283	8.7	6.486	–	–	–	–
Al 1	3944.006	–0.623	313.7	5.457	307.5	4.251	108.5	3.930	153.0	3.856
Al 1	3961.520	–0.323	259.3	4.986	258.6	3.797	96.1	3.488	117.5	3.032
Si 1	3905.523	–1.090	352.9	6.710	422.8	5.765	176.5	5.614	191.6	5.284
Si 1	4102.936	–3.140	–	–	–	–	–	–	59.5	5.068
Ca 1	4094.925	–1.736	50.7	6.880:	29.3	6.130:	8.6	5.718:	8.8	5.074:
Ca 1	4098.528	–1.579	–	–	36.7	6.112:	–	–	12.1	5.077:
Ca 1	4203.117	–0.923	21.1	5.708	21.5	5.484	4.2	4.923	7.3	4.619:
Ca 1	4226.728	0.265	–	–	–	–	198.1	4.166:	170.2	3.477:
Ca 1	4283.011	–0.292	110.1	6.173	97.1	5.258	50.0	4.890	47.9	3.931
Ca 1	4318.652	–0.295	99.0	6.004	86.3	5.135	44.1	4.759	42.1	3.838
Ca 1	4355.079	–2.544	67.3	8.129:	34.1	7.173:	8.5	6.669:	–	–
Ca 1	4425.437	–0.286	98.2	5.585	89.7	4.698	39.4	4.497	36.8	3.682
Ca 1	4434.957	0.066	124.0	5.540	118.6	4.585	58.8	4.475	57.1	3.725
Ca 1	4435.679	–0.412	95.4	5.670	79.7	4.731	32.8	4.494	41.9	3.908
Ca 1	4454.779	0.335	143.7	5.453	141.3	4.475	73.8	4.447	68.6	3.702
Ca 1	4455.887	–0.414	101.3	5.759	76.5	4.710	31.5	4.478	29.1	3.660
Ca 1	4456.616	–1.590	45.6	5.999	20.7	5.102	4.9	4.691	6.2	4.025
Ca 1	4526.928	–0.907	49.8	6.118	25.7	5.346	7.8	4.984	–	–
Ca 1	4578.551	–0.170	48.4	5.274	27.0	4.524	8.5	4.122:	8.3	3.452:
Ca 1	4685.268	–0.544	22.9	5.397	10.8	4.762	–	–	–	–
Sc 2	3567.696	–0.476	103.8	3.099	70.4	1.930	41.0	1.321	87.7	0.592
Sc 2	3576.340	0.007	129.9	3.005	101.2	1.914	66.6	1.611	125.7	1.043:
Sc 2	4246.822	0.242	131.1	2.769	93.3	1.699	67.3	1.450	114.6	0.600
Sc 2	4314.083	–0.096	113.3	3.068	76.4	2.060	38.3	1.297	91.3	0.679
Sc 2	4320.732	–0.252	92.7	2.829	53.9	1.765	28.0	1.175	73.3	0.365
Sc 2	4374.457	–0.418	92.1	3.004	55.0	1.974	24.3	1.256	68.0	0.424
Sc 2	4415.557	–0.668	85.2	3.068	48.8	2.060	15.1	1.192	53.5	0.344
.....										

A portion of the atlas comprising four stars is presented in graphical form in Figure 2 (normalized intensity, normalized to the continuum, versus laboratory wavelength). A complete set of atlas in electronic format for the wavelength range 3550–5000 Å is available at *http://www.chjaa.org*. Each individual graph covers 60 Å with overlapping of 20 Å. Some principal details used for the chemical composition calculation are identified.

5 STELLAR PARAMETERS

For comparison, the model atmospheric parameters determined by other investigators are given in Table 3. We present here our results of chemical abundance determination of these four stars along with their stellar parameters. We should note that these results are mere approximations, and we plan to determine in future more accurate values using a non-LTE code for some special chemical elements. The stellar parameters were

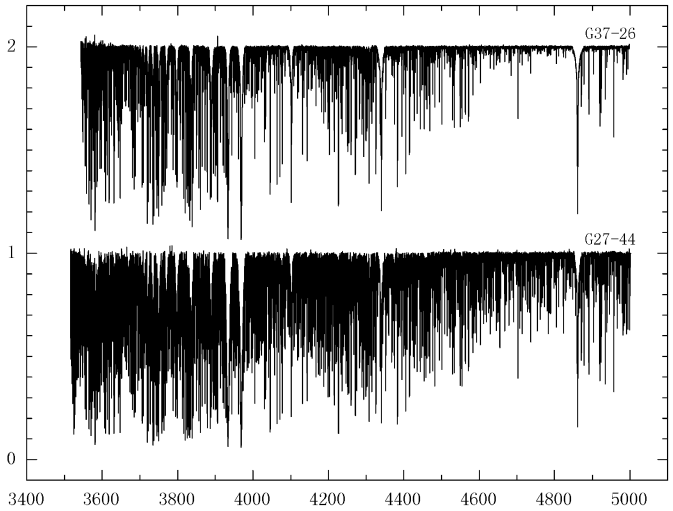

Fig. 1 Comparison of the spectra of two stars with very different metallicities (G37–26 ([Fe/H] = –2.04) and G27–44 ([Fe/H] = –0.60)) over the whole registered spectral region.

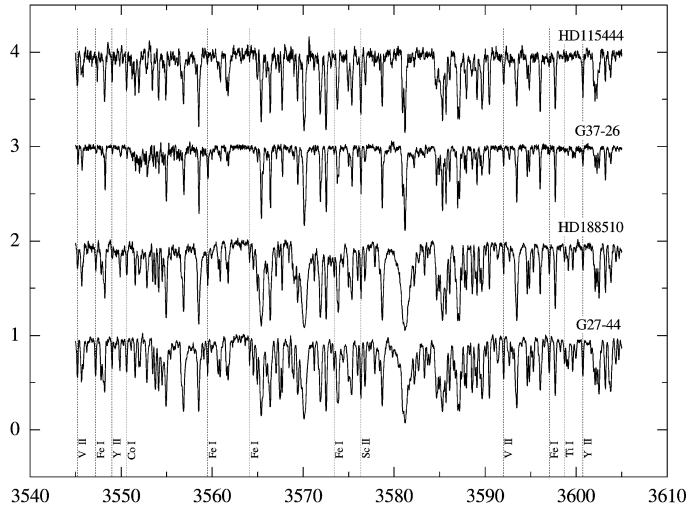

Fig. 2 Spectra of stars studied (from top to bottom: HD 115444 ([Fe/H]= -2.91), G37–26 ([Fe/H]= -2.04), HD 188510 ([Fe/H]= -1.52), G27–44 ([Fe/H]= -0.60). Some lines from Table 2 are marked with vertical lines.

determined in the following way. The effective temperature was derived using the Stromgren indices ($b-y$, c_1) from Hauck & Mermilliod (1998) and the calibration based on the method of infrared flux (Alonso et al. 1996, 1999). The metallicity values needed for the initial iteration of $T_{\rm eff}$ were taken from the published sources, but in the following iterations our spectroscopic [Fe/H] values were used. Moreover, this procedure was followed in different stars for between 100 and 230 FeI lines. Besides, to control the $T_{\rm eff}$ values we have added the generally adopted spectroscopic determinations of $T_{\rm eff}$, with a forced independence of $\lg\varepsilon$(Fe) on the low level excitation potentials. Figure 3 illustrates the method of $T_{\rm eff}$ for the star G37-26 (the adopted parameters are $T_{\rm eff} = 5890$ K, $\lg g = 4.50$ and $[{\rm Fe/H}] = -2.04$).

Table 3 Stellar Parameters Used by Previous Investigations

Star	$T_{\rm eff}$, K	$\lg g$	[Fe/H]	Reference
HD 188510	5450	–	–1.75	Carney et al. 1994
	5638	5.16	–1.37	Gratton et al. 1996
	5495	4.10	–1.70	Israelian et al. 1998
	5325	4.60	–1.60	Fulbrait 2000
G27–44	5759	–	–0.88	Carney et al. 1994
	5976	4.36	–0.65	Chen et al. 2001
	6002	4.45	–0.62	Gratton et al. 1996
G37–26	5842	–	–2.12	Carney et al. 1994
	6080	4.72	–1.88	Gratton et al. 1996
	5810	4.30	–2.15	Israelian et al. 1998
	6016	4.43	–1.95	Zhao & Gehren 2000
	5825	4.20	–2.00	Fulbrait 2000
HD 115444	–	–	–2.90	Carney et al. 1994
	4650	1.50	–2.99	Westin et al. 2000

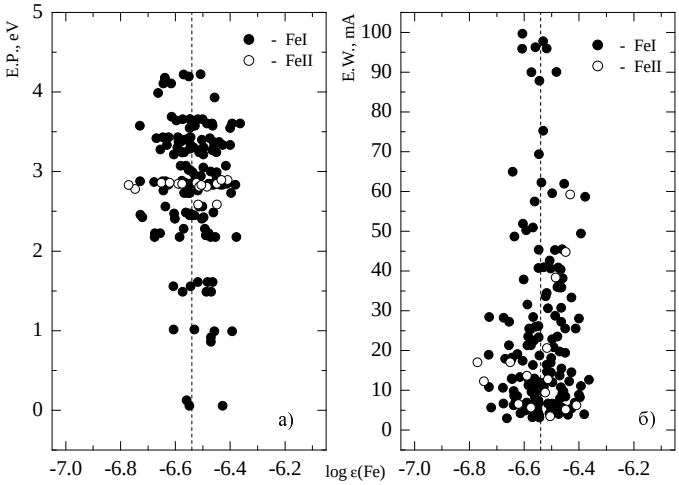

Fig. 3 a) To illustrate the method of effective temperature determination – neutral iron abundances calculated from individual lines as a function of their excitation potential; b) to illustrate the method of microturbulent velocity determination – neutral iron abundances calculated from individual lines as a function of their equivalent widths.

As a rule, a surface gravity is determined by the ionization balance, that is, a certain number of the elements obtained from lines of neutral and ionized atoms should be equal. However, the result may be affected by the following uncertainties: mistaken incorrect value of the oscillators strengths, non-LTE effects for the FeI lines, and error in the model atmospheric structure. Therefore, we calculate a surface gravity according to the well-known relation:

$$\lg \frac{g}{g_\odot} = \lg \frac{\mathcal{M}}{\mathcal{M}_\odot} + 4 \lg \frac{T_{\rm eff}}{T_{\rm eff_\odot}} + 0.4(M_{\rm bol} - M_{\rm bol,\odot}) \,,$$

where

$$M_{\rm bol} = V + BC + 5 \lg \pi + 5 \,,$$

$\mathcal{M}$ is the stellar mass, $M_{\rm bol}$ the bolometric luminosity, V the visual magnitude, BC the bolometric correction and π the stellar parallax. The Hipparcos parallaxes (ESA 1997) were used in the calculations. The stellar masses were determined using the evolution tracks of Vandenberg et al.(2000), given in steps of ≈ 0.1dex in metallicity. Bolometric corrections were calculated using the calibration formula from Balona (1994). The microturbulent velocity ξ_t was determined by forcing the neutral iron abundance to be independent of the equivalent width (E.W.) of the FeI line (see Fig. 3b). The programme WIDTH9 (Kurucz 1992) and the Kurucz's grid of the atmospheric models (Kurucz 1993) were used for the chemical abundance calculations.

6 CHEMICAL COMPOSITION

Lines with E.W. < 100 mÅ are usually used for chemical abundance determination for stronger lines are more sensitive to the choice of microturbulent velocity. Lines giving a systematic deviation in chemical content were not taken into account. In Table 4, the successive columns present, for the four program stars, the elemental species, solar abundance, result of abundances determination (average value $\lg\varepsilon$, the error of determination σ) and the number of lines used, N. The solar abundances are taken from Grevesse (1993). The relative abundances [X/Fe] for all elements are given in Table 5. The last column in Table 6 contains results for the star HD 115444 with abundance [X/Fe] by Westin et al. (2000) for common elements. Systematic deviation about 0.1 dex is caused by using different sets of oscillator strengths and adopted model parameters. It is seen that agreement is quite good including most of the heavy elements.

Table 4 Abundances of Chemical Elements ($\lg\varepsilon$) of Four Program Stars

Species	Sun	G27–44			HD 188510			G37–26			HD 115444		
	$\lg\varepsilon$	$\lg\varepsilon$	σ	N	$\lg\varepsilon$	σ	N	$\lg\varepsilon$	σ	N	$\lg\varepsilon$	σ	N
Na1	6.33	5.62	0.04	3	–			–			3.73	0.00	1
Mg1	7.58	7.14	0.08	7	6.33	0.07	6	6.09	0.05	5	5.44	0.06	5
Al1	6.47	5.23	0.24	2	4.03	0.23	2	3.71	0.22	2	3.45	0.42	2
Si1	7.55	6.71	0.00	1	5.76	0.00	1	5.61	0.00	1	5.18	0.11	2
Ca1	6.36	6.07	0.04	4	5.27	0.07	5	4.85	0.05	4	3.93	0.04	4
Sc2	3.17	2.95	0.05	8	1.90	0.05	8	1.32	0.05	8	0.49	0.05	7
Ti1	5.02	4.48	0.02	40	3.69	0.02	33	3.29	0.02	16	2.47	0.03	15
Ti2	5.02	4.62	0.02	31	3.82	0.02	22	3.34	0.02	24	2.52	0.02	31
V1	4.00	3.43	0.03	14	2.54	0.05	8	2.10	0.06	5	1.26	0.13	4
V2	4.00	3.72	0.04	7	2.73	0.09	5	2.09	0.08	4	1.27	0.04	4
Cr1	5.67	5.07	0.02	31	4.19	0.03	19	3.58	0.03	15	2.53	0.02	11
Cr2	5.67	5.28	0.04	11	4.33	0.03	6	3.78	0.05	7	2.99	0.07	5
Mn1	5.39	4.69	0.03	26	3.60	0.02	16	3.02	0.01	12	2.02	0.05	6
Fe1	7.50	6.91	0.01	231	5.98	0.01	200	5.47	0.01	149	4.59	0.01	105
Fe2	7.50	6.90	0.03	18	5.98	0.02	15	5.45	0.03	15	4.59	0.03	16
Co1	4.92	4.45	0.05	13	3.59	0.03	8	3.14	0.04	5	2.37	0.07	6
Ni1	6.25	5.57	0.01	37	4.69	0.02	22	4.12	0.02	12	3.34	0.03	11
Zn1	4.60	3.92	0.02	3	3.16	0.01	2	2.66	0.04	3	1.96	0.08	2
Sr2	2.90	2.27	0.12	3	1.03	0.10	2	1.02	0.10	3	0.06	0.04	2
Y2	2.24	1.74	0.07	7	0.72	0.02	7	0.21	0.04	7	-0.63	0.04	7
Zr2	2.60	2.06	0.04	5	1.51	0.08	5	0.92	0.07	5	0.04	0.05	7
Ba2	2.13	1.74	0.06	2	0.71	0.00	1	0.35	0.07	2	–0.06	0.17	2
La2	1.22	0.85	0.06	5	0.00	0.05	4	–			–1.36	0.05	5
Ce2	1.55	1.20	0.08	9	0.41	0.06	3	–0.12	0.03	2	–1.07	0.03	6
Nd2	1.50	1.35	0.05	7	0.71	0.08	6	–0.06	0.00	1	–0.81	0.04	7
Sm2	1.01	0.73	0.05	5	0.31	0.06	2	0.38	0.01	2	–1.13	0.05	7
Eu2	0.51	0.57	0.00	1	–0.25	0.00	1	–1.40	0.00	1	–1.14	0.00	1
Gd2	1.12	0.82	0.10	2	1.09	0.00	1	–			–0.83	0.08	2
Dy2	1.14	0.85	0.22	3	–			–0.33	0.00	1	–1.03	0.10	3

Table 5 Relative Abundances $[X/Fe]$ of Program Stars and Comparison with the Results of HD 155444 by Westin et al. (2000)

Species	G27–44	HD 188510	G37–26	HD 155444	HD 155444_{W2000}
Na1	–0.12	–	–	+0.30	0.00
Mg1	+0.16	+0.27	+0.55	+0.77	+0.54
Al1	–0.65	–0.93	–0.72	–0.12	–0.36
Si1	–0.24	–0.27	+0.11	+0.53	+0.46
Ca1	+0.31	+0.43	+0.53	+0.48	+0.38
Sc2	+0.37	+0.25	+0.19	+0.23	+0.17
Ti1	+0.06	+0.19	+0.31	+0.35	+0.47
Ti2	+0.20	+0.32	+0.37	+0.41	+0.45
V1	+0.03	+0.06	+0.14	+0.16	+0.16
V2	+0.32	+0.25	+0.13	+0.17	+0.15
Cr1	–0.01	+0.04	–0.05	–0.23	–0.28
Cr2	+0.20	+0.18	+0.16	+0.23	–
Mn1	–0.10	–0.27	–0.33	–0.47	–0.50
Fe1	+0.00	-0.00	+0.01	–0.00	+0.01
Fe2	–0.00	+0.00	–0.01	+0.00	–0.01
Co1	+0.13	+0.19	+0.27	+0.36	+0.31
Ni1	–0.09	–0.04	–0.09	–0.01	–0.01
Zn1	–0.08	+0.09	+0.10	+0.26	+0.25
Sr2	–0.03	–0.35	+0.16	+0.07	+0.32
Y2	+0.10	–0.00	+0.01	+0.04	–0.07
Zr2	+0.06	+0.43	+0.36	+0.35	+0.37
Ba2	+0.21	+0.10	+0.26	+0.72	+0.18
La2	+0.23	+0.30	–	+0.33	+0.37
Ce2	+0.25	+0.38	+0.37	+0.35	+0.34
Nd2	+0.45	+0.73	+0.48	+0.60	+0.56
Sm2	+0.31	+0.82	+1.41	+0.77	+0.81
Eu2	+0.66	+0.76	+0.14	+1.26	+0.85
Gd2	+0.30	+1.49	–	+0.96	+0.89
Dy2	+0.31	–	+0.57	+0.74	+0.88

For most of the stars we obtained their metallicities and other elemental abundances. We found, for example, that the α-process elements Mg, Ca, Ti are overabundant for stars with low metallicity. Figure 4 shows an example of this for the FeI lines measured in the spectra of G37–26. If we take into account only the lines with E.W. < 100 mÅ, we can exclude such effects on the average abundance of the element. An analysis of the effect is beyond the scope of this paper. We should like to note, however, that such deviation was found earlier (Klochkova et al. 1991) in the results of a spectroscopic study of stars in the galactic disk and a good explanation is yet to be found. It is evident that the deviation is not caused by the neglect of the damping effect (which would increase the abundances from strong lines). We can only declare that the accuracy of E.W. measurement in our work is not a main factor of error in the determination of the abundances.

Provided there is a sufficient number of spectral lines for the abundance calculation of a large number of elements, a short wavelength range is advantageous for the task of chemical composition determination. For the temperature and pressure of subdwarf atmospheres the coefficient of extinction in the continuum near 4000 Å is lower by about 0.2 dex than in the red part of the spectrum. It means that extinction in the continuum originates deeper in the atmosphere than that in the red range (near 6000 Å). Therefore, weak shorter-wavelength lines are formed on average closer to the photosphere than are the longer-wavelength lines. Hopefully, this means that a model description is more accurate for short-wavelength lines than for long-wavelength lines.

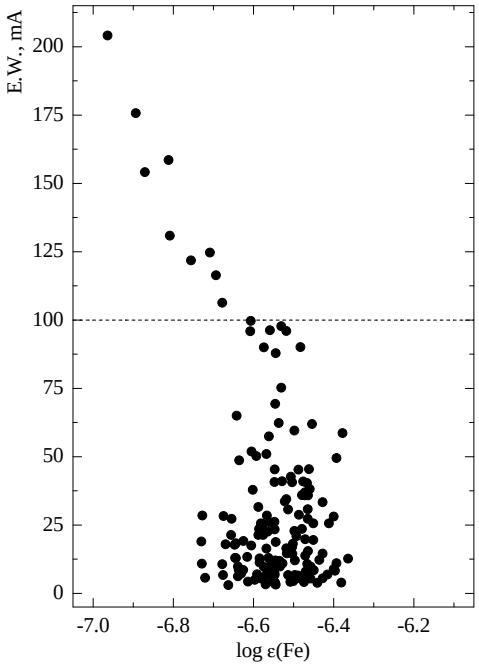

Fig. 4 Deviation from linearity of the "equivalent width – logarithm of abundance" plot for FeI lines with E.W.$>$ 100 mÅ in the spectrum of G37–26.

7 CONCLUSIONS

In this paper we make a comparative study of the spectra of a set of G – K-stars with very low metallicities. The spectral features are carefully found and identified in the range 3550–5000 Å. For the first time a unique atlas of spectra in UV and blue wavelengths ranges with a high spectral resolution $R = 60\,000$ is presented. Such an atlas is a tribute to the creation of an echelle spectrograph NES with a camera of fused silica and its implementation in the observing practice at the 6-meter telescope. Now we have a spectrograph NES that works in combination with a large CCD 2048$\times$2048 pixels ("Uppsala" CCD, Panchuk et al. 2002a) with a high sensitivity in a blue spectral range.

An atlas of halo stars is presented for the range 3550-5000 Å. The line identification was made using model atmospheres. The uncertainties in the chemical abundance determination of halo stars based on blue spectra are discussed. Use of the atlas is not confined only to the determination of chemical composition of halo stars. For example, it could be useful for line identification in the blue spectral range where the spectra of solar type stars are crowded and the line identification is difficult.

Acknowledgements This study is supported by the Russian Foundation for Basic Research (the project 05-07-90087), the RFBR+GFEN project 03-02-39019 and the National Natural Science Foundation of China under grant Nos. 10433010 and 10521001.

References

Alonso A., Arribas S., Martinez-Roger C., 1996, A&A, 313, 873
Alonso A., Arribas S., Martinez-Roger C., 1999, A&AS, 140, 261
Balona L. A., 1994, MNRAS, 268, 119
Beers T. C., Christlieb N., 2005, ARA&A, 43, 531
Carney B. W., Latham D. W., Laird J. B., Aguilar L. A., 1994, AJ, 107, 2240
Chen Y. Q., Nissen P. E., Benoni T., Zhao G., 2001, A&A, 371, 943

ESA 1997, The Hipparcos and Tycho Catalogues, ESA SP-1200
Fulbright J. P., 2000, AJ, 120, 1841
Galazutdinov G., Preprint Spec. Astrophys. Observ., 1992, No. 92
Gratton R. G., Carretta E., Castelli F., 1996, A&A, 314, 191
Grevesse N., 1993, The paper reported at d'Evry Schatzman Coll. "Physical Processes in Astrophysics" held at Paris Observ., Sept. 1993
Hauck B., Mermilliod M., 1998, A&AS, 129, 431
Israelian G., Lopez R. J. K., Rebolo R., 1998, ApJ, 507, 805
Klochkova V. G., Panchuk V. E., Tsymbal V. V., 1991, Bull. Special Astrophys. Observ., 33, 41
Kupka F., Piskunov N. E., Ryabchikova T. A. et al., 1999, A&AS, 138, 119
Kurucz R. L., 1992, In: The Stellar Population of Galaxies, eds., B. Barbuy, A. Renzini., IAU Symph., 149. p.225
Kurucz R. L., 1993, SAO. Cambridge, CDROM 13
Nissen P. E., In: High Resolution Spectroscopy with the VLT, ESO Conference and Workshop Proceedings No.40, 1992, p.49
Panchuk V. E., Klochkova V. G., Najdenov I. D., 1999, Preprint Bull. Special Astrophys. Observ., No. 135
Panchuk V. E., Piskunov N. E., Klochkova V. G. et al., 2002a, Preprint Bull. Special Astrophys. Observ., No. 169
Panchuk V. E., Klochkova V. G., Piskunov N. E. et al., 2002b, Preprint Bull. Special Astrophys. Observ., No. 170
Pierce A. K., Breckinridge J. B., 1974, The Kitt Peak table of photographic solar spectrum wavelength, Kitt Peak National Observatory Contribution, 559
Piskunov N. E., Kupka F., Ryabchikova T. A. et al., 1995, A&AS, 112, 525
Ryabchikova T. A., Piskunov N. E., Stempels H. C. et al., 1999, In: Proc. of the 6th International Colloquium on Atomic Spectra and Oscillator Strengths, Victoria BC. Canada. Physica Scripta, 83, 162
Tsymbal V. V., 1996, Model Atmospheres and Spectrum Synthesis, ASP Conf. Ser., 108, 198
VandenBerg D. A., Swenson F. J., Rogers F. J. et al., 2000, ApJ, 532, 430
Westin J., Sneden C., Gustafsson B. et al., 2000, ApJ, 530, 783
Zhao G., Gehren T. 2000, A&A, 362, 1077
Zhao G., Chen Y. Q., Shi J. R. et al., 2006, Chin. J. Astron. Astrophys. (ChJAA), 6, 265